Letter

Langdon effect in the realm of extreme ultraviolet source plasmas

J. Gonzalez [1] and J. Sheil [1,2,*]
[1] *Advanced Research Center for Nanolithography, Science Park 106, 1098 XG Amsterdam, The Netherlands*
[2] *Department of Physics and Astronomy, and LaserLaB, Vrije Universiteit Amsterdam, De Boelelaan 1081, 1081 HV Amsterdam, The Netherlands*

(Received 27 September 2024; accepted 7 January 2025; published 6 February 2025)

Already some years ago, Langdon [Phys. Rev. Lett. **44**, 575 (1980)] proposed that inverse bremsstrahlung absorption in plasmas drives free electrons into non-Maxwellian distributions. Radiation-hydrodynamic simulations of plasma-based light sources, however, often (implicitly) assume Maxwellian-distributed electrons. In this paper, we quantify the effect of non-Maxwellian distributions on laser absorption and thermal conduction in laser-driven plasma light sources. For irradiation conditions $I_{\rm las}\lambda_{\rm las}^2 \in [10^{11}, 10^{13}]\,{\rm W\,cm^{-2}\,\mu m^2}$ and plasma parameters $Z_{\rm eff}/T_e \in [0.2, 0.6]\,{\rm eV}^{-1}$, the electron distributions are predicted to be super-Gaussian of order $m \simeq$ 2.2–2.4. As a result, laser absorption is calculated to be 10–20% lower than plasmas with Maxwellian-distributed electrons. A ~10–30% reduction of the Spitzer-Härm thermal conduction coefficient is also predicted.

DOI: 10.1103/PhysRevE.111.L023201

Radiation-hydrodynamic (rad-hydro) simulations play a crucial role in the design and interpretation of laser-produced plasma (LPP) experiments, such as those encountered in inertial confinement fusion (ICF) research [1–3], as well as laser-plasma radiation sources for nanolithography [4–11] and biological imaging [12–14]. The basic principle in these latter two applications is the same: a target (such as Mo [15], Sn [16], Xe [17], W [18], or Au [19]) is irradiated with moderate-intensity laser pulses ($I_{\rm las} = 10^{10} - 10^{13}\,{\rm W\,cm^{-2}}$) to create plasmas that radiate intensely in application-specific wavelength regions. For nanolithography, this region is the 13.5 ± 0.135 nm band (the reflective wavelengths of molybdenum-silicon multilayer mirrors [20]) and for biological imaging interest lies in the water window region (2.3–4.4 nm) [12]. Identifying experimental conditions that maximize light source performance is a very challenging task, and it is here that predictive rad-hydro modeling can play a defining role.

While predictivity is an obvious criterion for any simulation capability, the many interacting components of rad-hydro simulations [21] (e.g., atomic kinetics [22,23], heat transport [24,25], and equation-of-state properties [26]), as well as their numerous possible implementations, complicates the testing and benchmarking of rad-hydro codes. An additional challenge arises when modeling laser absorption in a plasma. In 1980, Langdon [27] predicted that inverse bremsstrahlung absorption (IBA) drives free electrons into non-Maxwellian distributions so long as electron-electron collisions are not sufficiently frequent to establish a Maxwellian distribution. The effect is inherently nonlinear; preferential heating of low-energy electrons results in a lower laser absorptivity than plasmas with a Maxwellian electron distribution function (EDF). The number of electrons in the high-energy tail is also suppressed compared to a Maxwellian EDF; see Fig. 1 of Matte *et al.* [28]. A correction factor is typically incorporated into rad-hydro simulations to account for the reduction in laser absorption [8].

Only in the recent experimental works of Turnbull *et al.* [29] and Milder *et al.* [30–32] were non-Maxwellian EDFs identified in high-temperature, ICF-relevant laser-driven plasmas. The aforementioned reduction in laser absorption was observed in the work of Turnbull *et al.* [33], where a subsequent analysis [34] revealed that accounting for (i) the super-Gaussian nature of the EDFs in deriving the Coulomb logarithm and (ii) a correction for ion screening were necessary to bring calculations into agreement with measurements. An impression of the cumulative impact of their findings for hohlraum simulations is presented in Fig. 9 of Ref. [34], where a near halving of laser absorption is predicted. What is more, the presence of non-Maxwellian EDFs also modifies heat transport and atomic kinetics processes, the full consequences of which are currently unknown [35–38]. It is important to note that the underlying motivation for many of the aforementioned studies is fusion research, and it is not known how the findings presented therein translate to lower-temperature, laser-driven extreme ultraviolet (EUV), or soft x-ray light sources. It is the goal of the present work to make strides in this direction.

In this paper, we investigate the Langdon effect in the realm of laser-driven EUV light source plasmas. We know of two studies, those of Sunahara *et al.* [8,39], that account for the aforementioned reduction in laser absorption in EUV source simulations. While Scott *et al.* [21] acknowledge that the Langdon effect will become important for state-of-the-art CO_2-driven (laser wavelength $\lambda_{\rm las} = 10.6$ μm) plasmas [40], its impact on plasma properties and source performance was

*Contact author: j.sheil@arcnl.nl

not quantified. Moreover, we are unaware of any studies that have investigated the consequences of non-Maxwellian EDFs on thermal transport and atomic kinetics in EUV source plasmas. Our goal is to bridge these gaps; we provide theoretical evidence that non-Maxwellian EDFs will emerge in EUV source plasmas and, furthermore, we calculate the corrections to laser absorption and thermal conduction as a result of these non-Maxwellian EDFs. In light of the complete absence of EDF measurements in EUV source plasmas, we restrict our analysis to the framework described by Langdon [27], and postpone an investigation of the effects of non-Maxwellian distributions on the Coulomb logarithm [34,41] (needed for deriving the laser absorptivity) to future work.

The Langdon effect can be summarized as a distortion of the EDF into a non-Maxwellian one due to the preferential heating of low-energy electrons [27]. The "strength" of this distortion is characterized by the Langdon parameter α, which represents the ratio of the IBA heating rate to the electron-electron collision rate:

$$\alpha = Z_{\text{eff}} \frac{v_{\text{osc}}^2}{v_{th}^2} = 3.735 \times 10^{-13} I_{\text{las}} \lambda_{\text{las}}^2 \frac{Z_{\text{eff}}}{T_e}. \quad (1)$$

Here, $Z_{\text{eff}} = \langle Z^2 \rangle / \langle Z \rangle$ is the effective ionic charge, v_{osc} is the oscillation velocity of an electron in the electric field of the laser, v_{th} is the electron thermal velocity, and T_e is the electron temperature in eV. If α is small [27], for instance, then electron-electron collisions are sufficiently frequent to "counteract" IBA heating and a Maxwellian distribution is maintained. Langdon obtained the following form for the reduction in laser absorptivity:

$$f_L = 1 - \frac{0.553}{1 + (0.27/\alpha)^{0.75}}. \quad (2)$$

You see here two important features. As $\alpha \to 0$ (electron-electron collisions dominate), $f_L \to 1$; near-100% absorptivity. The opposite trend, $\alpha \to \infty$ (IBA dominates), gives an upper limit to the reduction $f_L \approx 1 - 0.553 = 0.447$. With increasing α, the EDF deviates further and further from a Maxwellian. Matte *et al.* [28] found that these distributions are well described by super-Gaussian functions of the form $f_e(v) \propto \exp[-(v/v_m)^m]$, where m is the order of the super-Gaussian, $v_m^2 \equiv \frac{3\Gamma(3/m)}{\Gamma(5/m)} v_{th}^2$, and Γ is the gamma function. They presented a scaling relation between m and α of the form

$$m = 2 + \frac{3}{1 + 1.66/\alpha^{0.724}}. \quad (3)$$

In the limiting cases $\alpha \to 0$, $m \to 2$ (a Maxwellian distribution) and $\alpha \to \infty$, $m \to 5$. This scaling relation was found to be in good agreement with experimental measurements [29,31,32,42].

To determine f_L and m in EUV source conditions, we must first identify appropriate values of Z_{eff}, I_{las}, λ_{las}, and T_e. We know from atomic kinetics considerations (see Ref. [43] and the references therein) that the 13.5 nm-emitting tin charge states $Z \in [11^+, 15^+]$ are bred in plasmas with $T_e \in [20, 50]$ eV. We therefore "restrict" the ratio Z_{eff}/T_e, appearing in Eq. (1), to lie in the range $Z_{\text{eff}}/T_e \in [0.2, 0.6]\,\text{eV}^{-1}$. Second, we know from the work of Hemminga *et al.* [44] that the optimum laser parameters (that is, the laser parameters that generate highly efficient EUV-emitting plasmas) scale according to $I_{\text{las}} = 1.44 \times 10^{11} \lambda_{\text{las}}^{-1}\,\text{W cm}^{-2}$ for $\lambda_{\text{las}} \in [1.064, 10.64]$ µm, and thus $I_{\text{las}} \lambda_{\text{las}}^2 = 1.44 \times 10^{11} \lambda_{\text{las}}\,\text{W cm}^{-2}\,\mu\text{m}^2$. As discussed in Hemminga *et al.* [44] and Gonzalez and Sheil [45], heating the plasma beyond the optimum laser intensity is a simple means of increasing EUV production. As a result, we fix $I_{\text{las}} \lambda_{\text{las}}^2$ to lie in the range $I_{\text{las}} \lambda_{\text{las}}^2 \in [10^{11}, 10^{13}]\,\text{W cm}^{-2}\,\mu\text{m}^2$. While these ranges were derived with laser-driven tin plasmas in mind, the conclusions presented below are valid for a broader range of plasma-based light sources.

The results of our calculations for f_L and m are shown in Figs. 1(a) and 1(b), respectively. The colormaps extend from $f_L = 0.5$, $m = 4$ (yellow) to $f_L = 1$, $m = 2$ (blue) and the white lines represent contours of fixed f_L and m. First, we consider plasmas driven by short-wavelength Nd:YAG ($\lambda_{\text{las}} = 1.064$ µm) and Tm:YLF ($\lambda_{\text{las}} = 2$ µm) lasers [44,46–49]. For the former, we have $I_{\text{las}} \lambda_{\text{las}}^2 \sim 1.4 \times 10^{11}\,\text{W cm}^{-2}\,\mu\text{m}^2$, giving $f_L \sim 0.95$ and $m \sim 2$; the reduction is rather minor, and the distributions remain close to Maxwellian. The Tm:YLF case is more interesting: $I_{\text{las}} \lambda_{\text{las}}^2 \sim 3 \times 10^{11}\,\text{W cm}^{-2}\,\mu\text{m}^2$, giving $f_L \sim 0.85$ and $m \sim 2.3$. You see here a strong sensitivity of the reduction factor to even slight deviations of the EDF from a Maxwellian. This reduction is further enhanced for CO_2-driven plasmas, where typical irradiation conditions $I_{\text{las}} \lambda_{\text{las}}^2 \sim 10^{12}\,\text{W cm}^{-2}\,\mu\text{m}^2$ gives $f_L \sim 0.8$ and $m \sim 2.4$. We should note that in our recent modeling of CO_2-driven plasmas [45], we did not account for this reduction in laser absorptivity, and this may contribute to differences between predicted and measured [40] conversion efficiencies. Regardless of the origin of this discrepancy, it is clear from the above that the Langdon effect should be incorporated into EUV source simulations.

It should also be remarked that the above analysis is based entirely on the frameworks of Langdon [27] and Matte *et al.* [28] We do not consider, for example, the effect of atomic kinetics on the EDF as was investigated in the recent work of Le *et al.* [38] Their inclusion of atomic kinetics processes in Vlasov-Boltzmann-Fokker-Planck (VBFP) simulations drove free electrons back toward a Maxwellian distribution, giving rise to a higher laser absorptivity (∼10%) than predicted by Eq. (2). While we expect that atomic kinetics processes will have a similar effect in EUV source plasmas, this remains to be confirmed.

Thermal conduction is another critical plasma process modified by the Langdon effect. Transport theories, such as the classical Spitzer-Härm (SH) formalism [50], assume Maxwellian-distributed electrons, where the tail of the distribution ($v > 3v_{th}$) is primarily responsible for heat transport [51]. The Langdon effect is thought to depopulate this high-energy tail, giving rise to a lower heat flux than predicted by SH theory [51]. For example, a near-40% reduction of the SH thermal conductivity is expected for an $m \simeq 3$ super-Gaussian distribution [35,51]. When calculating the heat flux in such situations, an additional complication arises in that the order of the super-Gaussian, m, varies in space. This leads to two additional terms in the non-Maxwellian heat flux: one due to gradients in electron density, ∇n_e, and the other due to

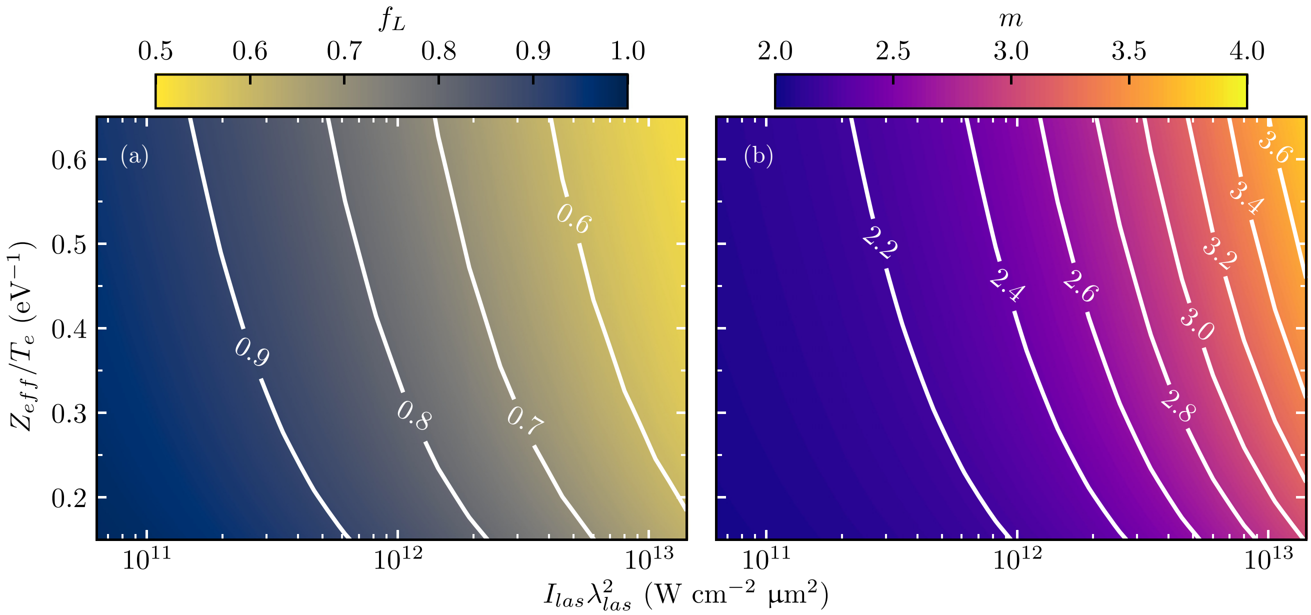

FIG. 1. (a) Langdon-induced reduction factor f_L and (b) super-Gaussian exponent m for the range of $I_{\rm las}\lambda_{\rm las}^2$ and $Z_{\rm eff}/T_e$ relevant for EUV source plasmas.

gradients in m, ∇m [35,52]:

$$Q_{\text{non-Max}} = -\left(C_T\kappa_{\rm SH}\nabla T_e + C_n\kappa_{\rm SH}T_e\frac{\nabla n_e}{n_e} + C_m\kappa_{\rm SH}T_e\frac{\nabla m}{m}\right). \quad (4)$$

Here, $\kappa_{\rm SH}$ is the SH thermal conduction coefficient [50], and C_T, C_n, and C_m are correction factors due to non-Maxwellian EDFs. The correction due to the density gradient, C_n, is close to 0 for all m (see Fig. 1 of Ref. [52]), and thus we neglect it in the following analysis. Expressions for C_T and C_m from Refs. [35,52] are

$$C_T = \frac{\Gamma\left(\frac{10}{m}\right)}{2}(7-5G)C, \quad (5)$$

$$C_m = \frac{\Gamma\left(\frac{10}{m}\right)}{2m}\left[35\psi\left(\frac{5}{m}\right) - 15\psi\left(\frac{3}{m}\right) - G\beta - 20\psi\left(\frac{10}{m}\right)\right]C, \quad (6)$$

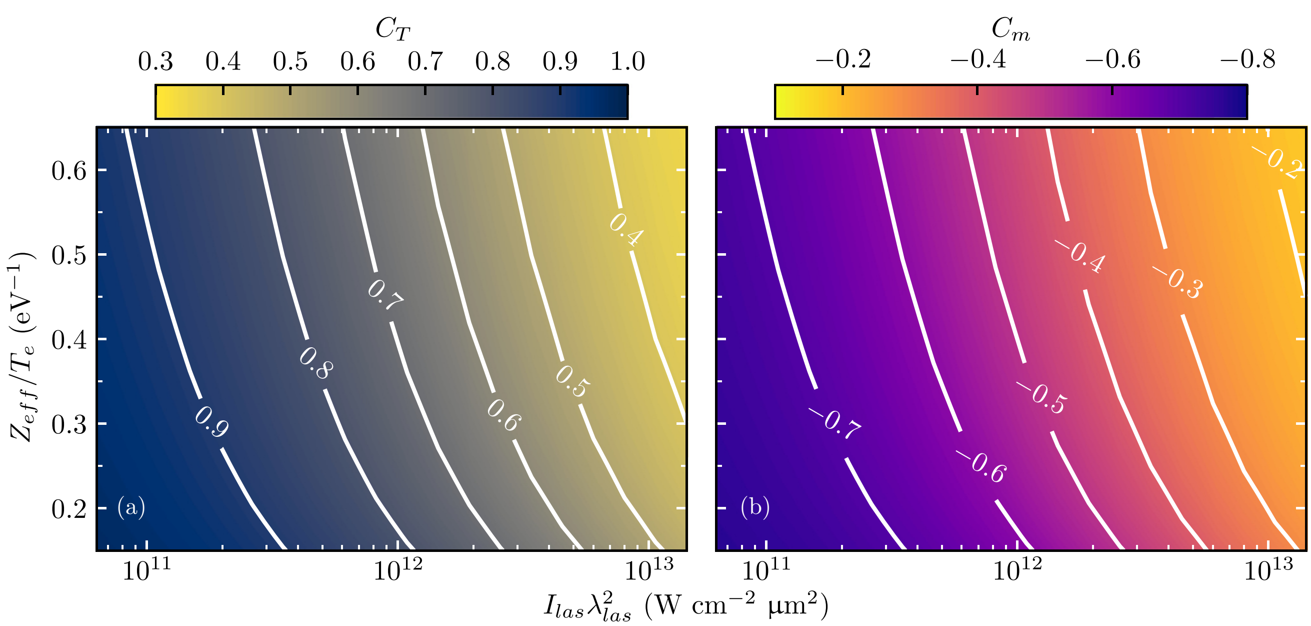

FIG. 2. Corrections to SH heat conductivity due to (a) temperature gradient (C_t) and (b) m gradient (C_m) in the relevant parameter range for LPP EUV sources.

where $C = \frac{\sqrt{\pi}}{48\Gamma(\frac{3}{m})}[\frac{3\Gamma(\frac{3}{m})}{2\Gamma(\frac{5}{m})}]^{\frac{7}{2}}$, $G = \frac{4[\Gamma(\frac{8}{m})]^2}{3\Gamma(\frac{6}{m})\Gamma(\frac{10}{m})}$, $\beta = 25\psi(\frac{5}{m}) - 9\psi(\frac{3}{m}) - 16\psi(\frac{8}{m})$, and $\psi(x) = \Gamma'(x)/\Gamma(x)$ is the polygamma function. All of these corrections depend on the plasma conditions implicitly through m. In Fig. 2, we present the corrections (a) C_T and (b) C_m, respectively, for EUV source conditions. Even for relatively low $I_{\rm las}\lambda_{\rm las}^2$ values, such as for Nd:YAG-driven plasmas, a near-10% reduction of the SH value is expected. These corrections are amplified for the CO_2-driven case: $C_T \sim 0.7$, a rather substantial correction. The correction C_m appearing in the ∇m term is everywhere negative and is similar in magnitude to C_T. Proper evaluation of these corrections in EUV source conditions requires proper modification of rad-hydro codes, such as that described in the ICF-relevant work of Huo *et al.* [35]. What is clear, however, is that the unique conditions associated with laser-driven EUV sources (that is, large values of $Z_{\rm eff}/T_e$ and laser wavelengths compared to ICF conditions) means that the Langdon effect can impact laser absorption and thermal conduction processes for laser intensities significantly lower than those typically used in ICF.

In conclusion, we have investigated the Langdon effect in the realm of EUV source plasmas. We have provided theoretical evidence that non-Maxwellian EDFs will emerge in these plasmas and modify both laser absorption and thermal conduction processes. It remains to be seen how these modifications alter our current understanding of laser-driven EUV sources. Proper evaluation of the EDF in these conditions, such as through VBFP simulations, would be very insightful. Experimental confirmation of the presence of non-Maxwellian EDFs in EUV source plasmas is also highly desirable. For example, modifying the Thomson scattering setup of Tomita *et al.* [53,54] and Pan *et al.* [55] to something akin to Milder *et al.* [31] could provide new, fundamental insights on plasma-based light sources. Going further, laser-driven EUV sources may provide a more easily accessible platform (compared to ICF platforms) for testing and refining theoretical predictions of the Langdon effect and, moreover, its impact on laser absorption, thermal conduction, and atomic kinetics processes.

We would like to thank H.A. Scott and A. Sunahara for useful discussions. This publication is part of the project ARIES with file number 20152 of the research programme VENI which is (partly) financed by the Dutch Research Council (NWO) under an NWO grant [56]. This work was conducted at the Advanced Research Center for Nanolithography, a public-private partnership between the University of Amsterdam, Vrije Universiteit Amsterdam, University of Groningen, the Netherlands Organization for Scientific Research (NWO), and the semiconductor equipment manufacturer ASML, and was (partly) financed by "Toeslag voor Topconsortia voor Kennis en Innovatie (TKI) from the Dutch Ministry of Economic Affairs."

[1] A. L. Kritcher, A. B. Zylstra, C. R. Weber, O. A. Hurricane, D. A. Callahan, D. S. Clark, L. Divol, D. E. Hinkel, K. Humbird, O. Jones, J. D. Lindl, S. Maclaren, D. J. Strozzi, C. V. Young, A. Allen, B. Bachmann, K. L. Baker, T. Braun, G. Brunton, D. T. Casey, T. Chapman, C. Choate, E. Dewald, J.-M. G. Di Nicola, M. J. Edwards, S. Haan, T. Fehrenbach, M. Hohenberger, E. Kur, B. Kustowski, C. Kong, O. L. Landen, D. Larson, B. J. MacGowan, M. Marinak, M. Millot, A. Nikroo, R. Nora, A. Pak, P. K. Patel, J. E. Ralph, M. Ratledge, M. S. Rubery, D. J. Schlossberg, S. M. Sepke, M. Stadermann, T. I. Suratwala, R. Tommasini, R. Town, B. Woodworth, B. Van Wonterghem, and C. Wild, Design of the first fusion experiment to achieve target energy gain $G > 1$, Phys. Rev. E **109**, 025204 (2024).

[2] O. S. Jones, L. J. Suter, H. A. Scott, M. A. Barrios, W. A. Farmer, S. B. Hansen, D. A. Liedahl, C. W. Mauche, A. S. Moore, M. D. Rosen, J. D. Salmonson, D. J. Strozzi, C. A. Thomas, and D. P. Turnbull, Progress towards a more predictive model for hohlraum radiation drive and symmetry, Phys. Plasmas **24**, 056312 (2017).

[3] B. M. Haines, D. E. Keller, K. P. Long, J. McKay, M. D., Z. J. Medin, H. Park, R. M. Rauenzahn, H. A. Scott, K. S. Anderson, T. J. B. Collins, L. M. Green, J. A. Marozas, P. W. McKenty, J. H. Peterson, E. L. Vold, C. Di Stefano, R. S. Lester, J. P. Sauppe, D. J. Stark, and J. Velechovsky, The development of a high-resolution Eulerian radiation-hydrodynamics simulation capability for laser-driven Hohlraums, Phys. Plasmas **29**, 083901 (2022).

[4] O. O. Versolato, Physics of laser-driven tin plasma sources of EUV radiation for nanolithography, Plasma Sources Sci. Technol. **28**, 083001 (2019).

[5] J. White, G. O'Sullivan, S. Zakharov, P. Choi, V. Zakharov, H. Nishimura, S. Fujioka, and K. Nishihara, Tin laser-produced plasma source modeling at 13.5 nm for extreme ultraviolet lithography, Appl. Phys. Lett. **92**, 151501 (2008).

[6] K. Nishihara, A. Sunahara, A. Sasaki, M. Nunami, H. Tanuma, S. Fujioka, Y. Shimada, K. Fujima, H. Furukawa, T. Kato, F. Koike, R. More, M. Murakami, T. Nishikawa, V. Zhakhovskii, K. Gamata, A. Takata, H. Ueda, H. Nishimura, Y. Izawa, N. Miyanaga, and K. Mima, Plasma physics and radiation hydrodynamics in developing an extreme ultraviolet light source for lithography, Phys. Plasmas **15**, 056708 (2008).

[7] A. Sunahara, A. Sasaki, and K. Nishihara, Two dimensional radiation hydrodynamic simulation for extreme ultra-violet emission from laser-produced tin plasmas, J. Phys.: Conf. Ser. **112**, 042048 (2008).

[8] A. Sunahara, K. Nishihara, and A. Sasaki, Optimization of extreme ultraviolet emission from laser-produced tin plasmas based on radiation hydrodynamics simulations, Plasma Fusion Res. **3**, 043 (2008).

[9] M. M. Basko, On the maximum conversion efficiency into the 13.5 nm extreme ultraviolet emission under a steady-state laser ablation of tin microspheres, Phys. Plasmas **23**, 083114 (2016).

[10] M. G. Su, Q. Min, S. Q. Cao, D. X. Sun, P. Hayden, G. O'Sullivan, and C. Z. Dong, Evolution analysis of EUV

radiation from laser-produced tin plasmas based on a radiation hydrodynamics model, Sci. Rep. **7**, 45212 (2017).

[11] T. Sizyuk and A. Hassanein, Tuning laser wavelength and pulse duration to improve the conversion efficiency and performance of EUV sources for nanolithography, Phys. Plasmas **27**, 103507 (2020).

[12] T. Higashiguchi, T. Otsuka, N. Yugami, W. Jiang, A. Endo, B. Li, P. Dunne, and G. O'Sullivan, Feasibility study of broadband efficient "water window" source, Appl. Phys. Lett. **100**, 014103 (2012).

[13] J. Wang, M. Kishimoto, T. Jozaki, T. Kumeda, T. Higashiguchi, A. Sunahara, H. Ohiro, K. Yamasaki, and S. Namba, Water-window x-ray emission from laser-produced Au plasma under optimal target thickness and focus conditions, Phys. Rev. E **107**, 065211 (2023).

[14] K. Mongey, S. J. J. de Lange, R. Brady, D. J. Hemminga, B. Delaney, M. M. Basko, E. Sokell, F. O'Reilly, and J. Sheil, Characterization of experimental and simulated micrometer-scale soft x-ray-emitting laser plasmas: Toward predictive radiance calculations, Appl. Phys. Lett. **124**, 102104 (2024).

[15] B. Li, T. Higashiguchi, T. Otsuka, W. Jiang, A. Endo, P. Dunne, and G. O'Sullivan, "Water window" sources: Selection based on the interplay of spectral properties and multilayer reflection bandwidth, Appl. Phys. Lett. **102**, 041117 (2013).

[16] S. Fujioka, M. Shimomura, Y. Shimada, S. Maeda, H. Sakaguchi, Y. Nakai, T. Aota, H. Nishimura, N. Ozaki, A. Sunahara, K. Nishihara, N. Miyanaga, Y. Izawa, and K. Mima, Pure-tin microdroplets irradiated with double laser pulses for efficient and minimum-mass extreme-ultraviolet light source production, Appl. Phys. Lett. **92**, 241502 (2008).

[17] H. Fiedorowicz, A. Bartnik, R. Jarocki, J. Kostecki, J. Krzywiński, J. Mikołajczyk, R. Rakowski, A. Szczurek, and M. Szczurek, Compact laser plasma EUV source based on a gas puff target for metrology applications, J. Alloys Compd. **401**, 99 (2005).

[18] A. Jonas, H. Stiel, L. Glöggler, D. Dahm, K. Dammer, B. Kanngießer, and I. Mantouvalou, Towards Poisson noise limited optical pump soft X-ray probe NEXAFS spectroscopy using a laser-produced plasma source, Opt. Express **27**, 36524 (2019).

[19] C. John, M. Kishimoto, T. Johzaki, T. Higashiguchi, N. Kakunaka, Y. Matsumoto, N. Hasegawa, M. Nishikino, T. Ejima, A. Sunahara, T. Endo, and S. Namba, Enhancement of water-window soft x-ray emission from laser-produced Au plasma under low-pressure nitrogen atmosphere, Opt. Lett. **44**, 1439 (2019).

[20] S. Bajt, J. B. Alameda, T. W. Barbee Jr., W. M. Clift, J. A. Folta, B. Kaufmann, and E. A. Spiller, Improved reflectance and stability of Mo/Si multilayers, Opt. Eng. **41**, 1797 (2002).

[21] H. Scott, S. Langer, and Y. Frank, Radiation-hydrodynamics modeling of LPP EUV sources, in *Photon Sources for Lithography and Metrology*, edited by V. Bakshi (SPIE Press, Washington, DC, 2023), pp. 71–110.

[22] S. B. Hansen, H.-K. Chung, C. J. Fontes, Y. Ralchenko, H. A. Scott, and E. Stambulchik, Review of the 10th Non-LTE code comparison workshop, High Energy Density Phys. **35**, 100693 (2020).

[23] Y. Ralchenko, Validation and verification of collisional-radiative models, in *Modern Methods in Collisional-Radiative Modeling of Plasmas*, edited by Y. Ralchenko (Springer International Publishing, Cham, 2016), pp. 181–208.

[24] P. E. Grabowski, S. B. Hansen, M. S. Murillo, L. G. Stanton, F. R. Graziani, A. B. Zylstra, S. D. Baalrud, P. Arnault, A. D. Baczewski, L. X. Benedict, C. Blancard, O. Čertík, J. Clérouin, L. A. Collins, S. Copeland, A. A. Correa, J. Dai, J. Daligault, M. P. Desjarlais, M. W. C. Dharma-wardana, G. Faussurier, J. Haack, T. Haxhimali, A. Hayes-Sterbenz, Y. Hou, S. X. Hu, D. Jensen, G. Jungman, G. Kagan, D. Kang, J. D. Kress, Q. Ma, M. Marciante, E. Meyer, R. E. Rudd, D. Saumon, L. Shulenburger, R. L. Singleton, T. Sjostrom, L. J. Stanek, C. E. Starrett, C. Ticknor, S. Valaitis, J. Venzke, and A. White, Review of the first charged-particle transport coefficient comparison workshop, High Energy Density Phys. **37**, 100905 (2020).

[25] L. J. Stanek, A. Kononov, S. B. Hansen, B. M. Haines, S. X. Hu, P. F. Knapp, M. S. Murillo, L. G. Stanton, H. D. Whitley, S. D. Baalrud, L. J. Babati, A. D. Baczewski, M. Bethkenhagen, A. Blanchet, Raymond C. Clay III, K. R. Cochrane, L. A. Collins, A. Dumi, G. Faussurier, M. French, Z. A. Johnson, V. V. Karasiev, S. Kumar, M. K. Lentz, C. A. Melton, K. A. Nichols, G. M. Petrov, V. Recoules, R. Redmer, G. Röpke, M. Schörner, N. R. Shaffer, V. Sharma, L. G. Silvestri, F. Soubiran, P. Suryanarayana, M. Tacu, J. P. Townsend, and A. J. White, Review of the second charged-particle transport coefficient code comparison workshop, Phys. Plasmas **31**, 052104 (2024).

[26] J. A. Gaffney, S. X. Hu, P. Arnault, A. Becker, L. X. Benedict, T. R. Boehly, P. M. Celliers, D. M. Ceperley, O. Čertík, J. Clérouin, G. W. Collins, L. A. Collins, J.-F. Danel, N. Desbiens, M. W. C. Dharma-wardana, Y. H. Ding, A. Fernandez-Pañella, M. C. Gregor, P. E. Grabowski, S. Hamel, S. B. Hansen, L. Harbour, X. T. He, D. D. Johnson, W. Kang, V. V. Karasiev, L. Kazandjian, M. D. Knudson, T. Ogitsu, C. Pierleoni, R. Piron, R. Redmer, G. Robert, D. Saumon, A. Shamp, T. Sjostrom, A. V. Smirnov, C. E. Starrett, P. A. Sterne, A. Wardlow, H. D. Whitley, B. Wilson, P. Zhang, and E. Zurek, A review of equation-of-state models for inertial confinement fusion materials, High Energy Density Phys. **28**, 7 (2018).

[27] A. B. Langdon, Nonlinear inverse bremsstrahlung and heated-electron distributions, Phys. Rev. Lett. **44**, 575 (1980).

[28] J. P. Matte, M. Lamoureux, C. Moller, R. Y. Yin, J. Delettrez, J. Virmont, and T. W. Johnston, Non-Maxwellian electron distributions and continuum X-ray emission in inverse bremsstrahlung heated plasmas, Plasma Phys. Control. Fusion **30**, 1665 (1988).

[29] D. Turnbull, A. Colaïtis, A. M. Hansen, A. L. Milder, J. P. Palastro, J. Katz, C. Dorrer, B. E. Kruschwitz, D. J. Strozzi, and D. H. Froula, Impact of the Langdon effect on crossed-beam energy transfer, Nat. Phys. **16**, 181 (2020).

[30] A. L. Milder, H. P. Le, M. Sherlock, P. Franke, J. Katz, S. T. Ivancic, J. L. Shaw, J. P. Palastro, A. M. Hansen, I. A. Begishev, W. Rozmus, and D. H. Froula, Evolution of the electron distribution function in the presence of inverse bremsstrahlung heating and collisional ionization, Phys. Rev. Lett. **124**, 025001 (2020).

[31] A. L. Milder, J. Katz, R. Boni, J. P. Palastro, M. Sherlock, W. Rozmus, and D. H. Froula, Statistical analysis of non-Maxwellian electron distribution functions measured with angularly resolved Thomson scattering, Phys. Plasmas **28**, 082102 (2021).

[32] A. L. Milder, J. Katz, R. Boni, J. P. Palastro, M. Sherlock, W. Rozmus, and D. H. Froula, Measurements of non-Maxwellian electron distribution functions and their effect on laser heating, Phys. Rev. Lett. **127**, 015001 (2021).
[33] D. Turnbull, J. Katz, M. Sherlock, L. Divol, N. R. Shaffer, D. J. Strozzi, A. Colaïtis, D. H. Edgell, R. K. Follett, K. R. McMillen, P. Michel, A. L. Milder, and D. H. Froula, Inverse bremsstrahlung absorption, Phys. Rev. Lett. **130**, 145103 (2023).
[34] D. Turnbull, J. Katz, M. Sherlock, A. L. Milder, M. S. Cho, L. Divol, N. R. Shaffer, D. J. Strozzi, P. Michel, and D. H. Froula, Reconciling calculations and measurements of inverse bremsstrahlung absorption, Phys. Plasmas **31**, 063304 (2024).
[35] W. Yi Huo, K. Lan, P. Jun Gu, H. Yong, and Q. Hong Zeng, Electron heat conduction under non-Maxwellian distribution in hohlraum simulation, Phys. Plasmas **19**, 012313 (2012).
[36] N. R. Shaffer, A. V. Maximov, and V. N. Goncharov, Thermal conductivity of a laser plasma, Phys. Rev. E **108**, 045205 (2023).
[37] N. R. Shaffer, M. Sherlock, A. V. Maximov, and V. N. Goncharov, An extended Vlasov-Fokker-Planck approach for kinetic simulations of laser plasmas, Phys. Plasmas **30**, 043906 (2023).
[38] H. P. Le, M. Sherlock, and H. A. Scott, Influence of atomic kinetics on inverse bremsstrahlung heating and nonlocal thermal transport, Phys. Rev. E **100**, 013202 (2019).
[39] A. Sunahara, A. Hassanein, K. Tomita, S. Namba, and T. Higashiguchi, Optimization of extreme ultra-violet light emitted from the CO_2 laser-irradiated tin plasmas using 2D radiation hydrodynamic simulations, Opt. Express **31**, 31780 (2023).
[40] I. Fomenkov, D. Brandt, A. Ershov, A. Schafgans, Y. Tao, G. Vaschenko, S. Rokitski, M. Kats, M. Vargas, M. Purvis, R. Rafac, B. La Fontaine, S. De Dea, A. LaForge, J. Stewart, S. Chang, M. Graham, D. Riggs, T. Taylor, M. Abraham, and D. Brown, Light sources for high-volume manufacturing EUV lithography: technology, performance, and power scaling, Adv. Opt. Techn. **6**, 173 (2017).
[41] M. Sherlock, P. Michel, D. J. Strozzi, L. Divol, E. Kur, and G. Zimmerman, Inverse bremsstrahlung absorption rate for super-Gaussian electron distribution functions including plasma screening, Phys. Rev. E **109**, 055201 (2024).
[42] J. M. Liu, J. S. De Groot, J. P. Matte, T. W. Johnston, and R. P. Drake, Measurements of inverse bremsstrahlung absorption and non-Maxwellian electron velocity distributions, Phys. Rev. Lett. **72**, 2717 (1994).
[43] J. Sheil, O. O. Versolato, V. Bakshi, and H. A. Scott, Review of the 1st EUV light sources code comparison workshop, Atoms **11**, 130 (2023).
[44] D. J. Hemminga, O. O. Versolato, and J. Sheil, Simulations of plasmas driven by laser wavelengths in the 1.064-10.6 μm range for their characterization as future extreme ultraviolet light sources, Phys. Plasmas **30**, 033301 (2023).
[45] J. Gonzalez and J. Sheil, On the role of target mass in extreme ultraviolet light generation from CO_2-driven tin plasmas for nanolithography, Phys. Plasmas **31**, 050701 (2024).
[46] R. Schupp, F. Torretti, R. A. Meijer, M. Bayraktar, J. Scheers, D. Kurilovich, A. Bayerle, K. S. E. Eikema, S. Witte, W. Ubachs, R. Hoekstra, and O. O. Versolato, Efficient generation of extreme ultraviolet light from Nd:YAG-driven microdroplet-tin plasma, Phys. Rev. Appl. **12**, 014010 (2019).
[47] S. Langer, C. Siders, T. Galvin, H. Scott, and E. Sistrunk, Simulations of EUV sources driven by CO_2 and thulium lasers, in *Source Workshop*, S94 (EUV Litho Inc., Texas, 2019).
[48] L. Behnke, R. Schupp, Z. Bouza, M. Bayraktar, Z. Mazzotta, R. Meijer, J. Sheil, S. Witte, W. Ubachs, R. Hoekstra, and O. O. Versolato, Extreme ultraviolet light from a tin plasma driven by a 2-μm-wavelength laser, Opt. Express **29**, 4475 (2021).
[49] I. Tamer, B. A. Reagan, T. Galvin, J. Galbraith, E. Sistrunk, A. Church, G. Huete, H. Neurath, and T. Spinka, Demonstration of a compact, multi-joule, diode-pumped Tm:YLF laser, Opt. Lett. **46**, 5096 (2021).
[50] L. Spitzer and R. Härm, Transport phenomena in a completely ionized gas, Phys. Rev. **89**, 977 (1953).
[51] P. Mora and H. Yahi, Thermal heat-flux reduction in laser-produced plasmas, Phys. Rev. A **26**, 2259 (1982).
[52] K. Li and W. Y. Huo, Nonlocal electron heat transport under the non-Maxwellian distribution function, Phys. Plasmas **27**, 062705 (2020).
[53] K. Tomita, Y. Sato, S. Tsukiyama, T. Eguchi, K. Uchino, K. Kouge, H. Tomuro, T. Yanagida, Y. Wada, M. Kunushima, G. Soumagne, T. Kodama, H. Mizoguchi, A. Sunahara, and K. Nishihara, Time-resolved two-dimensional profiles of electron density and temperature of laser-produced tin plasmas for extreme-ultraviolet lithography light sources, Sci. Rep. **7**, 12328 (2017).
[54] K. Tomita, Y. Pan, A. Sunahara, K. Kouge, H. Mizoguchi, and K. Nishihara, Observation of plasma inflows in laser-produced Sn plasma and their contribution to extreme-ultraviolet light output enhancement, Sci. Rep. **13**, 1825 (2023).
[55] Y. Pan, K. Tomita, A. Sunahara, A. Sasaki, and K. Nishihara, Joint measurement of electron density, temperature, and emission spectrum of Nd:YAG laser-produced tin plasma, Appl. Phys. Lett. **123**, 204103 (2023).
[56] https://www.nwo.nl/calls/nwo-talentprogramma-veni-ttw-2024.